



# Adsorptive removal of strontium(II) using macroporous poly(AGE-*co*-EGDMA) beads modified with resorcin[4]arene

K MULANI<sup>1</sup>, V PATIL<sup>2</sup>, N CHAVAN<sup>3</sup> and K DONDE<sup>1,\*</sup>

<sup>1</sup>Department of Chemistry, Ramnarain Ruia College, Matunga (E), Mumbai 400019, India

<sup>2</sup>Department of Chemistry, University of Mumbai, Vidyanaigari, Santacruz (E), Mumbai 400098, India

<sup>3</sup>Polymer Science and Engineering Division, CSIR-National Chemical Laboratory, Pune 411008, India

\*Author for correspondence (nitudonde@yahoo.co.in)

MS received 10 March 2018; accepted 24 October 2018; published online 9 March 2019

**Abstract.** Adsorption behaviour of strontium(II) on macroporous poly(allyl glycidyl methacrylate-*co*-ethylene glycol dimethacrylate) [poly(AGE-*co*-EGDMA)] beads modified with resorcin[4]arene was studied using macroporous cross-linked [poly(AGE-*co*-EGDMA)] beads. The macroporous crosslinked [poly(AGE-*co*-EGDMA)] beads were synthesized by suspension polymerization techniques, followed by functionalization with amino derivatives of resorcin[4]arene. The poly(AGE-*co*-EGDMA) beads were characterized by FTIR, <sup>1</sup>H and <sup>13</sup>C-NMR, elemental analysis and particle-size analysis. The surface morphology of beads was studied by scanning electron microscopy. The functionalized poly(AGE-*co*-EGDMA) beads were used as adsorbents for strontium removal. The crucial factors including the effect of pH, time, initial concentration of metal ions and adsorbent dose were investigated to optimize the maximum adsorption efficiency of Sr(II). The equilibrium data of strontium(II) ions adsorbed on functionalized poly(AGE-*co*-EGDMA) beads were analysed by pseudo-first- and pseudo-second-order kinetic models. The pseudo-second-order kinetic model indicated that strontium was adsorbed by chemisorption.

**Keywords.** AGE-EGDMA beads; resorcin[4]arene; Sr(II); adsorption.

## 1. Introduction

Presence of toxic metals in ground water sources is an important issue in water and wastewater treatments, which affects human health. It is surprising that nature has been a large producer of radioactive waste. Small amounts of radioactive materials are contained in mineral springs, sand mounds and volcanic eruptions. These are referred as naturally occurring radioactive materials (NORMs) and nuclear waste generated from nuclear reactors.

Nowadays, strontium is readily used in electronic industries because it improves brilliance of glass and the quality of picture. In the human body, teeth and bones were found to have the highest concentration of strontium. The most common health effects of radioactive <sup>90</sup>Sr include bone pain, bone fractures, bone disorders and bone cancer [1]. Since <sup>90</sup>Sr is considered to be one of the most hazardous elements in the fission product, it is necessary to remove it from the waste stream before being discharged to the environment.

There are several methods and technologies available for waste-water treatment. But unfortunately, not all processes and technologies are environmentally, economically and socially sustainable. The four major classes of chemical separation techniques of heavy metal recovery from waste water include chemical precipitation, solvent extraction, electrolytic recovery and adsorption/ion exchange.

Adsorption is one of the most efficient and advanced waste-water treatment methods that has been extensively used. Research on adsorption of strontium from drinking water has been explored. Adsorption is the most preferred method for the removal of strontium due to its low cost, versatility, economical effectiveness and simple usage. In the adsorption process, a substrate (adsorbate) is adsorbed on the adsorbing material (adsorbent). The most common adsorbent efficiently used for the treatment of waste water includes activated carbon, clay, minerals, bio-adsorbents, like algae, fungi, bacteria and yeast, and low cost adsorbents/agricultural waste [2–5].

Recently polymeric beads prepared by suspension polymerization techniques have extensively been used for metal-ion recovery due to their high surface area, porosity, mechanical and thermal stabilities. Due to their stability in a range of buffers from pH 1 to 11, acrylic-based resins are efficiently used as adsorbents for the removal of different metal ions [6]. However, microspheres have a higher packing density than the bulk material, and hence, hyper cross-linked polystyrene microspheres have been widely used as packing materials, adsorbents, templates for nanoparticle growth and ion exchange resins [7]. Zhou *et al* [8] systematically synthesized conjugated microporous polymers of tunable pore size distribution using different types of monomers. The functional polymers, like poly(vinyl pyridine–ethylene

glycol methacrylate–ethylene glycol dimethacrylate), have been synthesized and used for the removal of several metals [9]. Kurczewska and Schroeder [10] developed a novel complexing agent by modification of epoxy-based resin with a chelating agent i.e., amines for adsorption of metal ions from aqueous solutions.

In recent years, allyl glycidyl ether (AGE)-based macroporous cross-linked polymeric beads have attracted great interest because of their chemical and structural versatilities. The epoxy groups present in the AGE polymers can rapidly react with various reagents like amines, alcohols and thiols yielding a specific adsorbent with high capacity and good selectivity [11]. In this work, we report the synthesis of polymeric beads by suspension polymerization of AGE and ethylene glycol dimethacrylate (EGDMA). The functionalization of AGE-EGDMA beads was carried out using amino resorcin[4]arene. The resulting polymeric beads were used to study the adsorption capacity towards strontium metal.

## 2. Experimental

### 2.1 Materials

Analytical grade AGE and EGDMA were procured from Sigma-Aldrich, USA. Resorcinol, strontium nitrate, arsenazo(III), sodium citrate and sorbitan monooleate (Span 80) were purchased from Loba Chemie, Mumbai, India. Formaldehyde (37% solution) was received from Qualigens, India. Sulphuric acid (95–98%) and nitric acid (70%) were procured from Merck, India. The protecting colloid polyvinyl pyrrolidone (PVP, Mw 3,60,000 g mol<sup>-1</sup>) was obtained from Fluka Germany.

### 2.2 Preparation of polymeric beads

Polymeric beads (AGE-EGDMA) were prepared by copolymerization of AGE and EGDMA monomers by suspension polymerization techniques. The monomer composition is shown in table 1. The suspension polymerization was carried out in a double-walled cylindrical reactor with a diameter of 11 cm and a height of 15 cm. The continuous phase was prepared by dissolving 1% polyvinyl pyrrolidone in 100 ml of deionized water. The organic phase consisted of monomer AGE, crosslinker EGDMA, initiator AIBN and pore-forming agent, cyclohexanol. The organic phase was slowly added to the aqueous phase with a stirring speed of 300 rpm under a nitrogen atmosphere. After completion of addition, temperature was raised up to 70°C and polymerization was continued for 3 h.

The polymeric beads obtained were then thoroughly washed with water, methanol and acetone and dried overnight at 60°C under vacuum. Furthermore, polymeric beads were purified by the Soxhlet extraction method in which methanol was used as the extracting solvent. The scheme for the

**Table 1.** Monomer composition for the preparation of polymeric beads.

Polymer code	AGE in g (mol)	EGDMA in g (mol)	CLD, %
AE-25	6.278 (0.0550)	2.616 (0.0132)	25
AE-50	4.817 (0.0422)	4.202 (0.0212)	50
AE-75	3.949 (0.0346)	5.035 (0.0254)	75
AE-100	3.344 (0.0293)	5.807 (0.0293)	100
AE-150	2.556 (0.0224)	6.660 (0.0336)	150
AE-200	2.066 (0.0181)	7.195 (0.0363)	200

Monomer (O) phase: Monomer (AGE)+cross-linker(EGDMA)+Span 80= 1.6 g, AIBN=0.2 g, outer aqueous (W<sub>2</sub>) phase: water = 100 ml + PVP = 1 g, porogen = cyclohexanol, monomer to porogen ratio 1:1.6, stirring speed during polymerization = 300 rpm, polymerization temperature = 70°C, time = 3 h.

synthesis of polymeric beads of AGE-EGDMA is depicted in scheme 1.

### 2.3 Synthesis of resorcin[4]arene

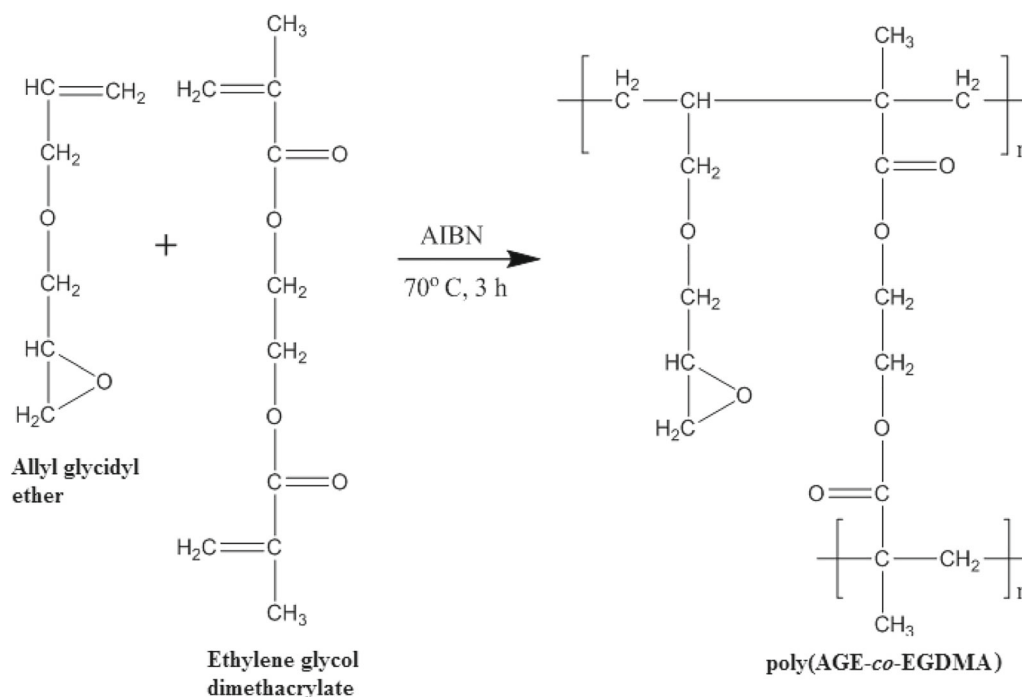
Resorcin[4]arene was synthesized according to a well-known procedure [12]. In a 100 ml two-necked round-bottom flask equipped with a reflux condenser and dropping funnel, 11 g (0.1 mol) of resorcinol and 12.6 ml (0.1 mol) of 35% acetaldehyde were added. The mixture was stirred for 15 min at 10°C. To the above reaction mixture, concentrated hydrochloric acid was carefully added with the help of a dropping funnel. The precipitate was rapidly formed. The reaction mixture was further stirred at 75°C for 1 h, cooled in an ice bath and filtered, and then washed with water. It was then recrystallized using ethanol:water (30:70) to obtain yellow coloured crystals of resorcin[4]arene. The synthesis of resorcin[4]arene and its amino derivatives are presented in scheme 2.

### 2.4 Aminomethylation of resorcin[4]arene

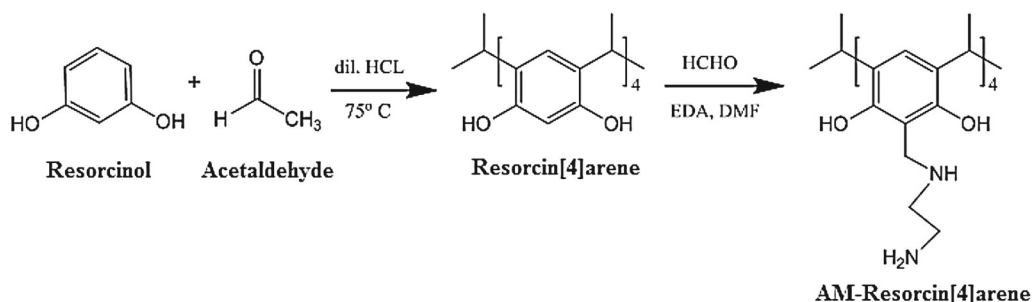
To a solution of 1 g (1.8 mmol) of resorcin[4]arene and 10 ml of ethanol:DCM (50:50), 360 μl (2.29 mmol) of formaldehyde and 240 μl (4.5 mmol) of ethylene diamine were added. The solution was stirred at room temperature for 12 h under a nitrogen atmosphere. Reaction progress was monitored by TLC in ethylacetate:chloroform (50:50). The product obtained was filtered and washed with methanol and dried at 60°C for 4 h [13].

### 2.5 Post-modification of AGE-EGDMA beads with amino resorcin[4]arene

In the reaction flask containing a mixture of 1,4-dioxane and deionized water (1:1 v/v), 2 g of AGE-EGDMA beads were added. To the above reaction mixture, sodium hydroxide and amino-methylated resorcin[4]arene were added. The reaction mixture was then refluxed at 80°C for 12 h. The resulting product was filtered and washed repeatedly with



**Scheme 1.** Preparation of AGE-EGDMA polymeric beads by the suspension polymerization of poly(AGE-co-EGDMA).



**Scheme 2.** Synthesis of resorcin[4]arene and its amino derivatives (AM-resorcin[4]arene).

distilled water. Finally, modified AGE-EGDMA beads were dried in a vacuum oven at 60°C. The post-modification of AGE-co-EGDMA is presented in scheme 3.

### 3. Results and discussion

#### 3.1 Determination of epoxy number

Ten millilitres of methanolic KOH was pipetted and titrated against standard 0.1 N KHP solution using phenolphthalein as an indicator. The end point is pink to colourless.

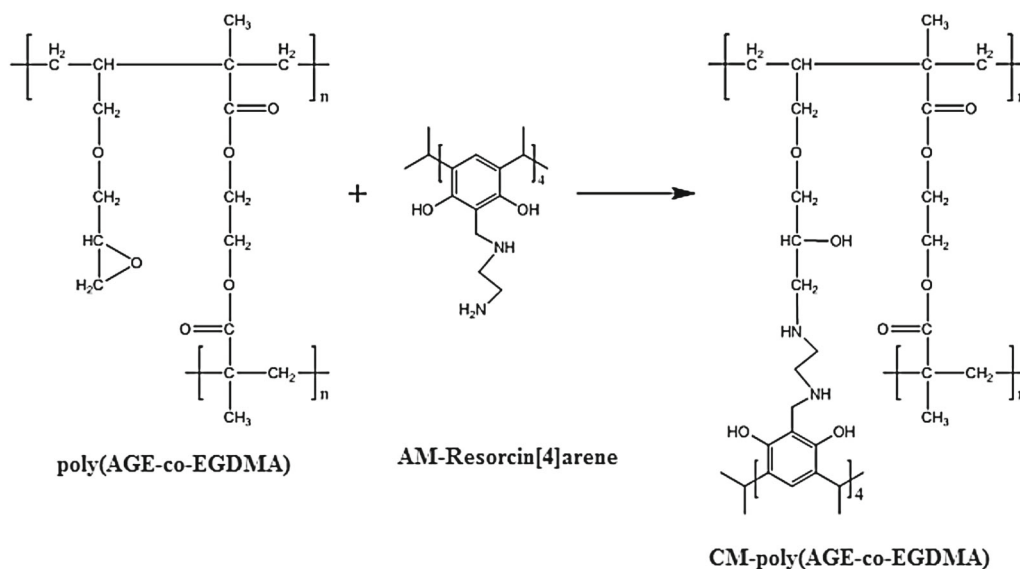
For the blank titration, 25 ml of pure 1,4-dioxane and 25 ml of 0.2 N HCl in dioxane solution were added in a conical flask and the solution was refluxed for 1, 3 and 6 h at 100–105°C. Then, flask was cooled to room temperature and 25 ml of

neutral cresol-red indicator was added. The reaction mixture was titrated against 0.1 N methanolic KOH. The end point is faint pink to violet.

The blank titration was carried out by weighing accurately 0.1 g of sample in a conical flask. To this conical flask, 25 ml of pure 1,4-dioxane and 25 ml of 0.2 N HCl in dioxane solution were added and the solution was refluxed for 1, 3 and 6 h at 100–105°C. Then, the flask was cooled to room temperature and 25 ml of neutral cresol-red indicator was added. The reaction mixture was titrated against 0.1 N methanolic KOH. The end point is faint pink to violet.

$$\text{Epoxy content} = \frac{(B - V) \times N}{10 \times W},$$

where  $B$  the volume (ml) of KOH standard aqueous solution consumed by HCl–dioxane solution with no dissolved



**Scheme 3.** Chemical modification of AGE-co-EGDMA beads with AM-resorcin[4]arene (CM-poly(AGE-co-EGDMA)).

**Table 2.** Epoxy content of AGE-EGDMA polymers.

Polymer code	AE-25	AE-50	AE-75	AE-100	AE-150	AE-200
Epoxy content (mmol g <sup>-1</sup> )	4.76	3.98	2.86	2.67	2.08	1.18

sample,  $V$  the volume (ml) of KOH standard aqueous solution consumed by HCl–dioxane solution with dissolved sample,  $N$  the normality of KOH and  $W$  the mass (g) of the sample.

To estimate the availability of surface epoxy groups, wet reactive epoxy titration was carried out. The epoxy content of AGE-EGDMA polymeric beads is summarized in table 2. The results show that epoxy content gradually decreases as cross-link density increases. Also, surface tension of AGE in contact with water is comparatively lower than that of EGDMA. Therefore, AGE molecules will tend to migrate towards the surface of droplets.

### 3.2 NMR spectroscopy

The <sup>1</sup>H and <sup>13</sup>C-NMR spectra of the resorcin[4]arene are shown in figures 1 and 2, respectively. The <sup>1</sup>H spectrum was recorded at 200 MHz in acetone-d<sub>6</sub> in the range of 0–14 ppm using tetramethylsilane as an internal standard.

The <sup>1</sup>H spectrum was recorded at 200 MHz in acetone-d<sub>6</sub> as shown in figure 1. Predominant sharp peaks are observed at  $\delta$  1.75 ppm (–CH<sub>3</sub>),  $\delta$  4.5 ppm (–CH–),  $\delta$  6.23 ppm (Ar–H),  $\delta$  7.66 and 8.68 ppm (Ar–OH) [14].

The <sup>13</sup>C spectrum was recorded at 200 MHz in acetone-d<sub>6</sub> as depicted in figure 2. The sharp peaks are observed at  $\delta$  20.5 ppm (–CH<sub>3</sub>),  $\delta$  103.8 ppm (–CH–),  $\delta$  125.4, 126.4 and 152.6 ppm (aromatic carbon).

The <sup>1</sup>H and <sup>13</sup>C-NMR spectra of the aminomethylated resorcin[4]arene are shown in figures 3 and 4, respectively, and <sup>13</sup>C-NMR depth is shown in figure 5.

The <sup>1</sup>H-NMR spectrum shows the predominant sharp peaks at  $\delta$  1.22 ppm (–CH<sub>2</sub>–),  $\delta$  1.70 ppm (–CH<sub>3</sub>),  $\delta$  3.70 ppm (Ar–CH<sub>2</sub>–),  $\delta$  4.56 ppm (–CH–),  $\delta$  6.23 ppm (Ar–H) and  $\delta$  8.12 ppm (Ar–OH).

The <sup>13</sup>C-NMR spectrum displayed the major peaks at  $\delta$  19.5 ppm (–CH<sub>3</sub>),  $\delta$  27.5 ppm (–CH<sub>2</sub>–),  $\delta$  44.2 ppm (N–CH<sub>2</sub>–),  $\delta$  56.6 ppm (Ar–CH<sub>2</sub>–),  $\delta$  107.8 ppm (–CH–),  $\delta$  121.5 and 124.8 ppm (aromatic carbon). In figure 5, the peak observed at  $\delta$  56.8 ppm is due to the formation of a methylene bridge.

### 3.3 Elemental analysis

The elemental composition of aminomethylated resorcin[4]arene-modified AGE-EGDMA polymeric beads is shown in table 3. This study reveals that AGE-EGDMA polymeric beads were chemically modified by aminomethylated resorcin[4]arene.

### 3.4 FTIR spectroscopy

The FTIR spectra of poly(AGE-EGDMA) beads and aminomethylated resorcin[4]arene-modified poly(AGE-EGDMA) beads are shown in figure 6. As seen in figure 6, the

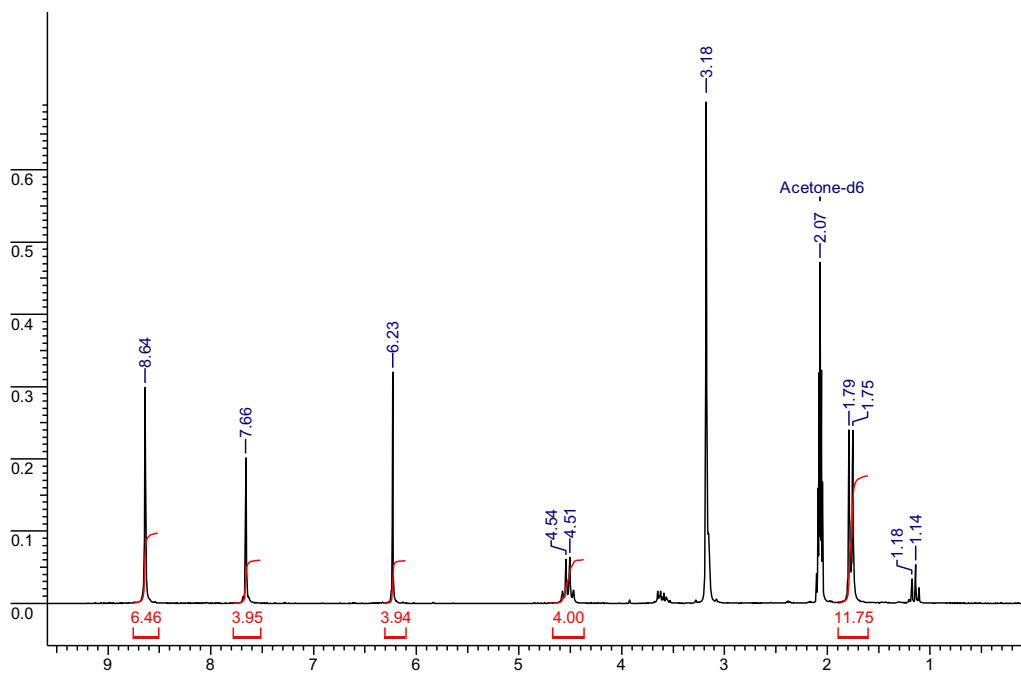


**Figure 1.**  $^1\text{H}$ -NMR resorcin[4]arene.

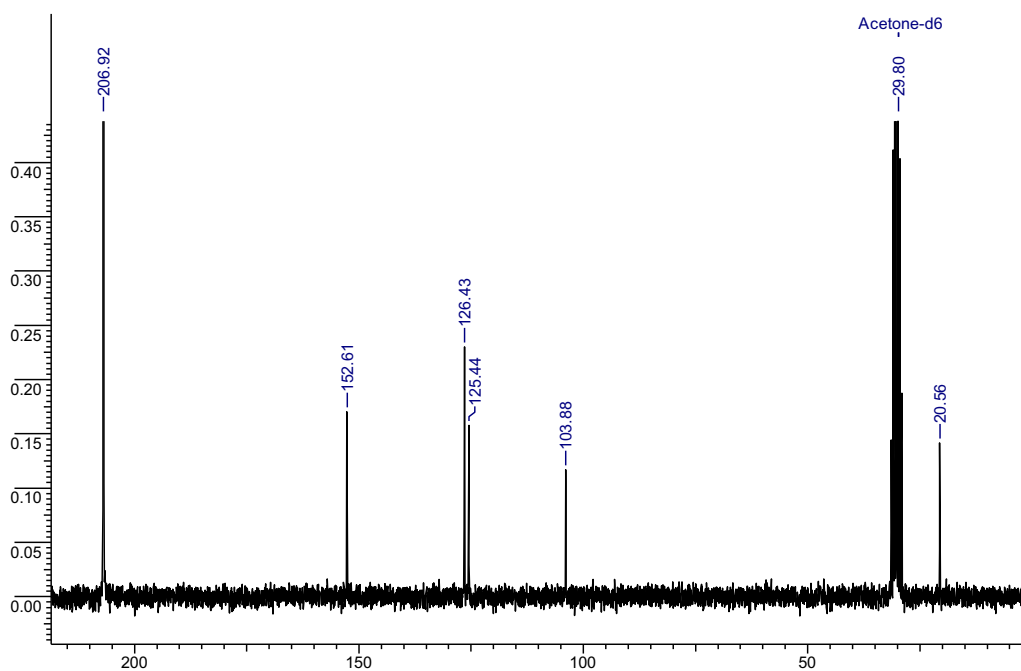


**Figure 2.**  $^{13}\text{C}$ -NMR resorcin[4]arene.

peak at  $968\text{ cm}^{-1}$  indicates the epoxy group incorporated into the polymer chain. The peak observed at  $2936\text{--}2991\text{ cm}^{-1}$  is assigned to the stretching vibration of the C–H bond. The peak displayed at  $1151\text{ cm}^{-1}$  is attributed to the stretching vibration of the C–O ester bond. The peak noticed at  $1730\text{ cm}^{-1}$  corresponds to the stretching vibration of the C=O bond.

The characteristic peaks for crosslinked AGE-EGDMA polymers were not changed in chemically modified beads, except for the intensity of the epoxy group vibration. The peaks observed at  $955$  and  $854\text{ cm}^{-1}$  attributed to the epoxy group vibration in the IR spectrum of poly(AGE-EGDMA) beads, which have not completely vanished in

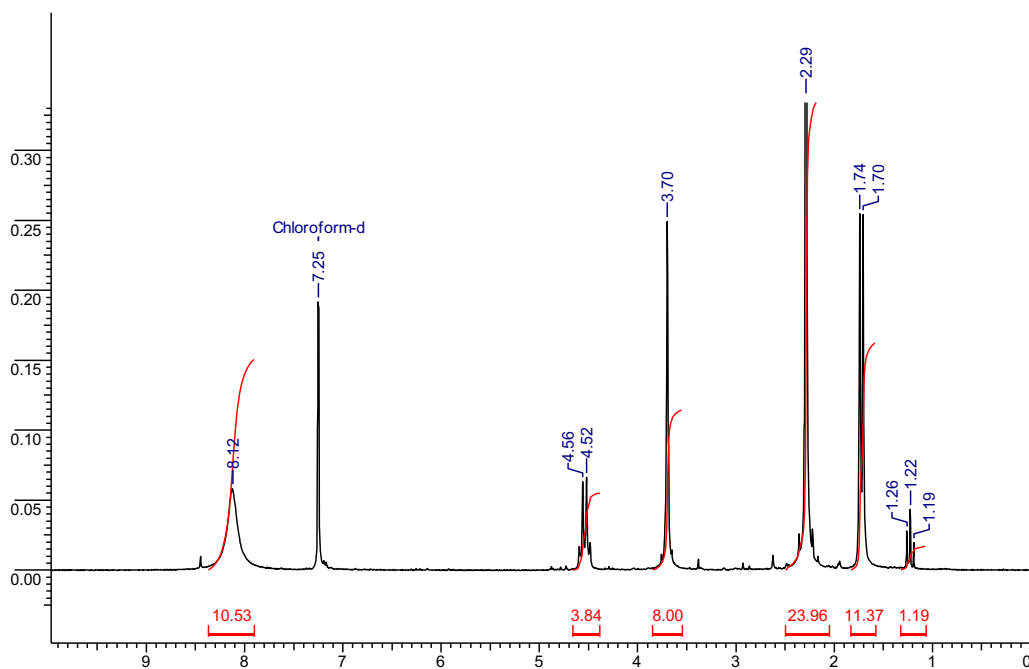


**Figure 3.**  $^1\text{H-NMR}$  of aminomethylated resorcin[4]arene.

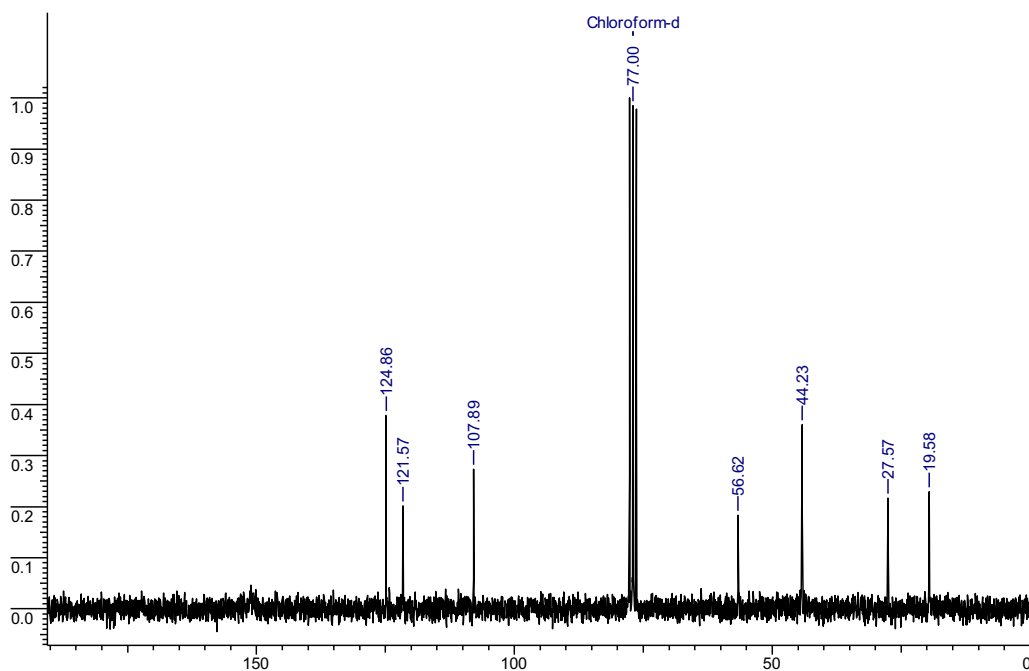


**Figure 4.**  $^{13}\text{C-NMR}$  of aminomethylated resorcin[4]arene.

chemically modified poly(AGE-EGDMA) beads, but their intensity became small and they were shifted to a higher frequency of  $968\text{ cm}^{-1}$ . The absorption peak at  $3528\text{ cm}^{-1}$  is assigned to the N–H stretching.

### 3.5 Surface morphology

The scanning electron microscopy images are used to visualize the surface morphology of the polymeric beads. The

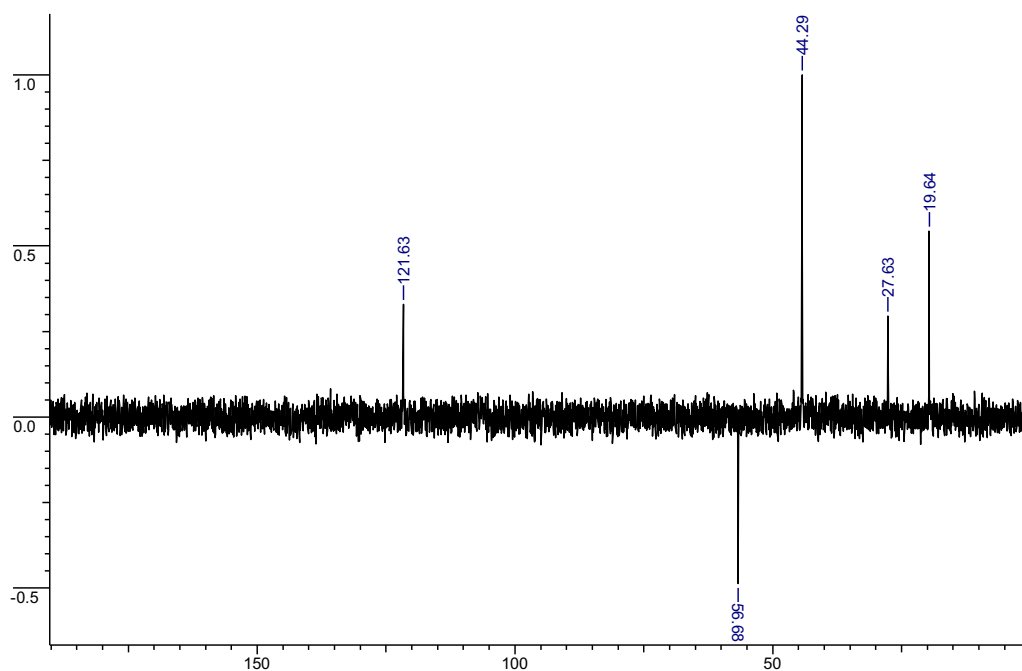


**Figure 5.**  $^{13}\text{C}$ -NMR of aminomethylated resorcin[4]arene (depth).

**Table 3.** Elemental composition of chemically modified AGE-EGDMA polymers.

Polymer code	% C	% H	% N
AE-25	56.95	6.94	0.85
AE-50	56.76	6.69	0.49
AE-75	56.41	6.34	0.45
AE-100	57.39	6.76	0.42
AE-150	56.91	6.32	0.32
AE-200	57.06	6.49	0.23

SEM images of AGE-EGDMA polymeric beads are shown in figure 7. It clearly indicates that the beads are spherical and monodisperse.

The surface morphology and properties of polymeric beads synthesized by suspension polymerization depend on the composition of the monomeric mixture and polymerization conditions. The initiator decomposes into free radicals. These free radicals initiate the polymerization and simultaneously cross-linking reaction takes place between the monomer and cross-linker. After certain reaction time, a three-dimensional network of infinitely large size may start to form beads. The surface area and pore volume of the synthesized AGE-EGDMA polymeric beads were measured by using a monosorb surface area analyser (Quantachrome Instruments, USA) and a single point Brunauer–Emmett–Teller method by measuring the adsorption of nitrogen at liquid nitrogen temperature. The experimental values obtained are presented in table 4. The surface area of AGE-EGDMA polymeric beads was in the range of 8–19  $\text{m}^2 \text{g}^{-1}$  which is relatively lower.

It may be due to water droplets or porogen droplets that are trapped during the formation of a cross-linking polymer. It also varies with the cross-link density. The pore volume of AGE-EGDMA polymeric beads was in the range of 0.033–0.076  $\text{cc g}^{-1}$ .

### 3.6 Particle size analysis

From several decades, a suspension polymerization technique was used to synthesize micro-sized polymeric beads for adsorption purposes. The polymers were produced with different morphologies and surface areas by changing porogen. These synthesized porous polymers are widely used in water-treatment operations. The column diagram of particle size distribution and average particle size, specific surface area and pore volume of AGE-EGDMA polymeric beads is shown in figure 8 and table 4, respectively.

### 3.7 Epoxy content

The concentration of the monomer and crosslinker (cross-link density) was determined by the following equation.

$$A = \frac{\text{Mol. wt. of } M}{\text{Density of } M} X + \frac{\text{Mol. wt. of } C}{\text{Density of } C} X_{\text{CLD}},$$

where  $A$  is the batch size,  $M$  the monomer,  $C$  the crosslinker, CLD the cross-link density and  $X$  the determination factor.

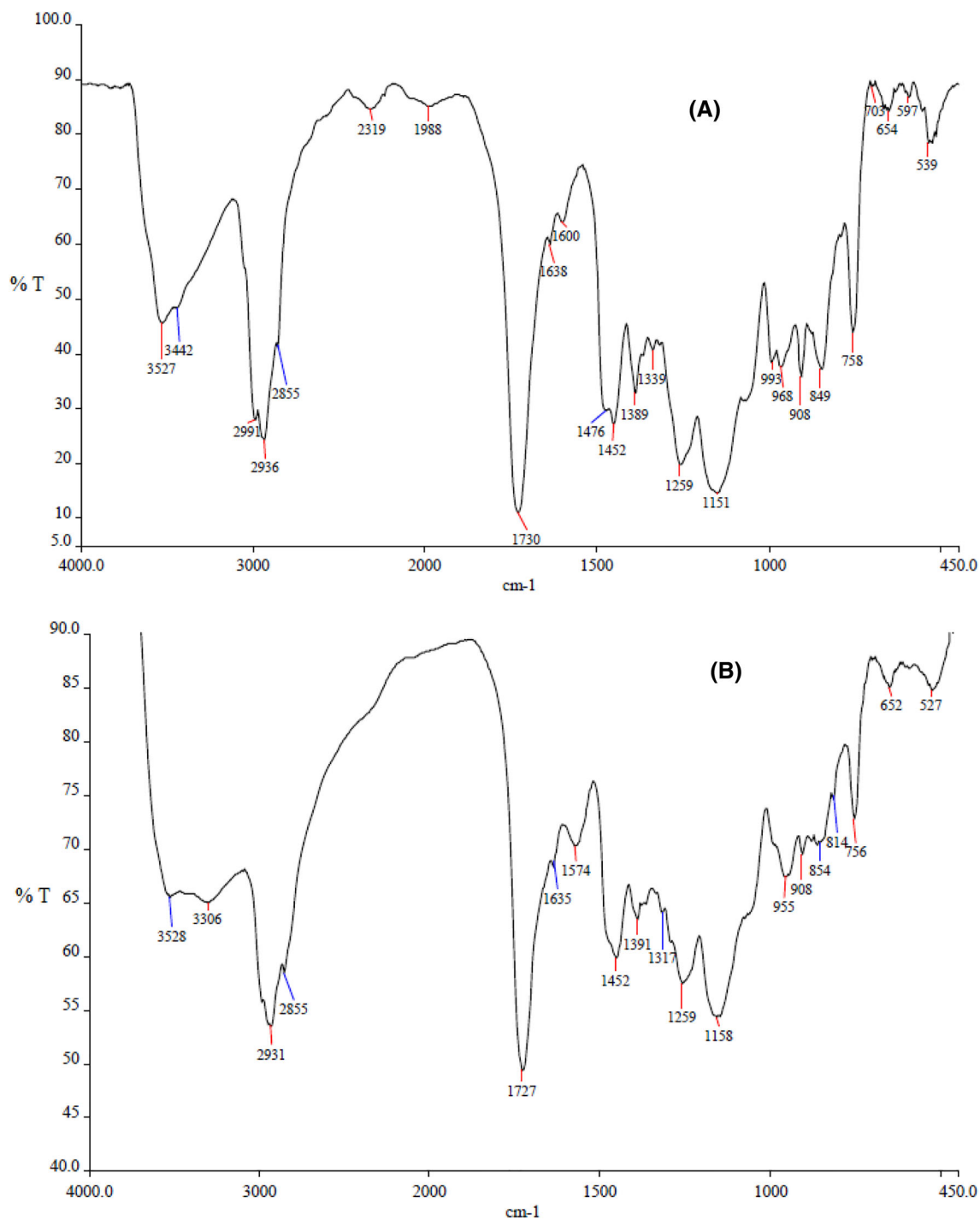


**Figure 6.** (A) FTIR spectrum of AGE-EGDMA beads and (B) modified AGE-EGDMA beads.

The surface epoxy content of AGE-EGDMA polymeric beads was determined by the titration method. The wet-reactive epoxy titration gives rough calculation of the availability of epoxy groups present on the polymer surface.

Figure 9 depicts the value of calculated and observed surface epoxy groups at different cross-link densities. It clearly indicates that the observed epoxy content was lower than

the calculated value. This may be due to the concentration of epoxy groups present at or near the surface, which react with acid during titration and is rather low. It indicates that the majority of epoxy groups were buried in the matrix. Hence, the observed epoxy value was lower compared to the calculated epoxy value. The epoxy value also decreases as cross-link density increases because the



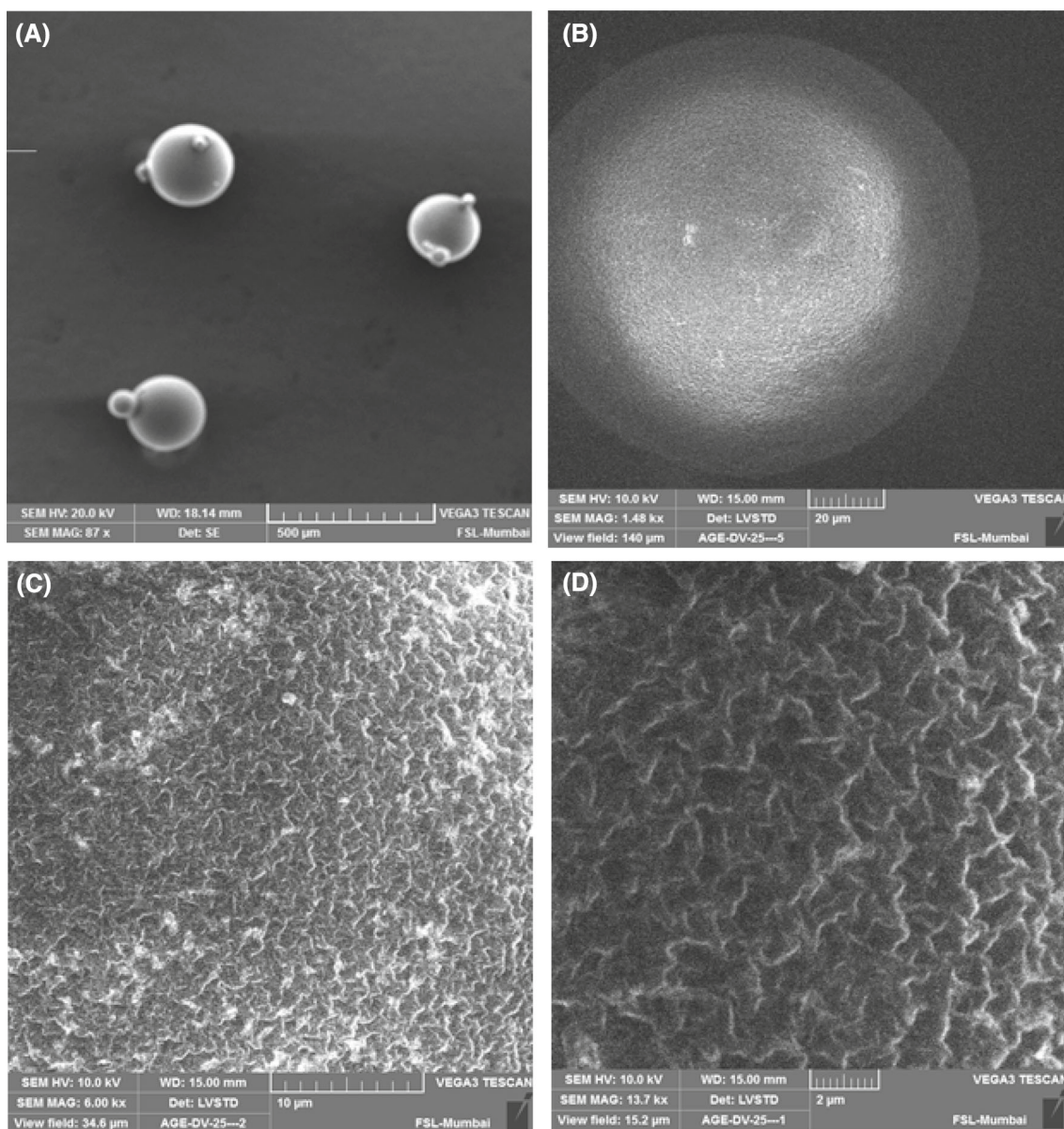


**Figure 7.** SEM images of AGE-EGDMA beads.

**Table 4.** Average particle size, specific surface area and pore volume of AGE-EGDMA polymeric beads.

Polymer code	Average particle size (μm)	Specific surface area (m <sup>2</sup> g <sup>-1</sup> )	Pore volume (cc g <sup>-1</sup> )
AE-25	89.12	10.72	0.035
AE-50	73.55	19.01	0.076
AE-75	73.45	13.66	0.047
AE-100	74.30	8.66	0.036
AE-150	88.97	18.21	0.070
AE-200	105.42	13.25	0.033

concentration of the AGE monomer decreases with an increase in cross-link density. The calculated epoxy value decreases with a decrease in AGE content in the polymer

varying from 6.19 to 1.96 mmol g<sup>-1</sup> (from 25 to 200% cross-link density). This is due to epoxy functionality which plays an important role in epoxidation. The epoxy values obtained by the titration method (experimental) are in the range of 4.76–1.18 mmol g<sup>-1</sup> (from 25 to 200% cross-link density). The difference between these epoxy values indicated that some fraction of the epoxy group undergo ring opening reaction and some fraction of the epoxy group in the polymeric beads were buried in the matrix.

### 3.8 Adsorption experiments

The synthesized aminoresorcin[4]arene-modified AGE-EGDMA polymeric beads were tested for the adsorption of strontium metal. In a sorption study, known quantity of

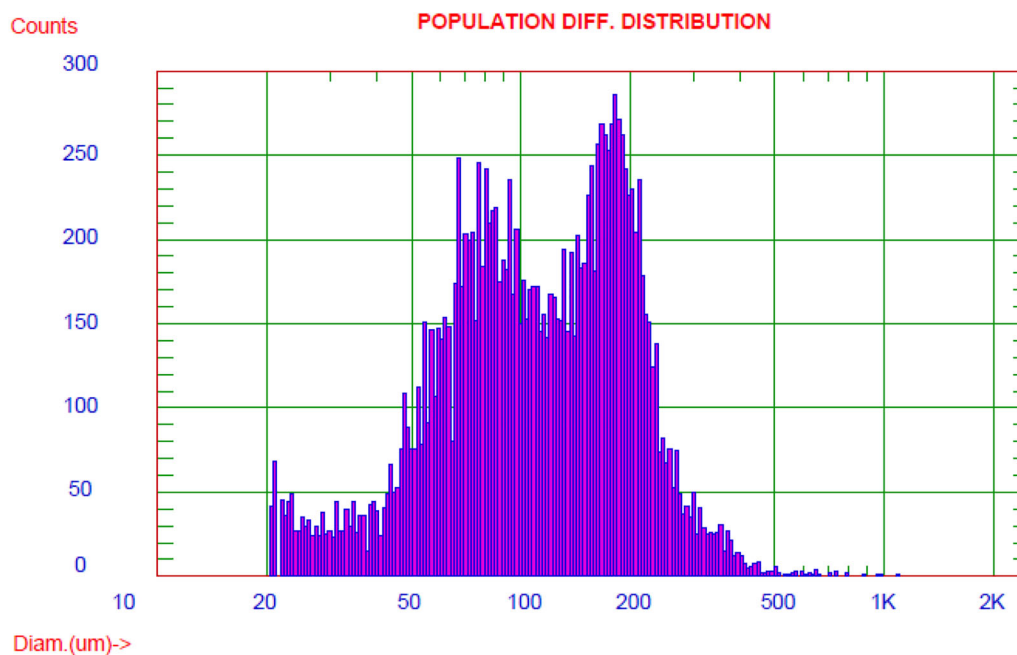


**Figure 8.** Column diagram of particle-size distribution of AE-25.

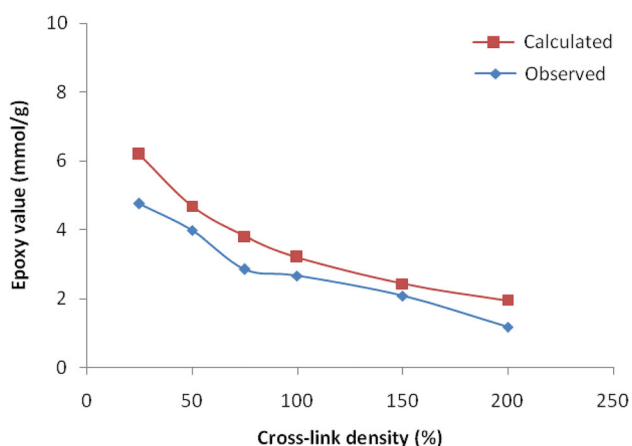


**Figure 9.** Comparison of surface epoxy contents (calculated and observed).

chemically modified AGE-EGDMA polymeric beads was gently shaken with known quantity of metal ion solution. The residual amount was spectrophotometrically analysed using the complexing agent arsenazo(III). Absorbance of the purple coloured solution was observed at  $\lambda$  640 nm against blank. All the experiments related to the adsorption study were carried out at room temperature.

The 100 ppm concentration of strontium chloride stock solution was prepared by dissolving 243.9 mg of strontium chloride in deionized water. From this, different concentration solutions were prepared to study the effect of concentration on metal adsorption. The complexing agent arsenazo(III)

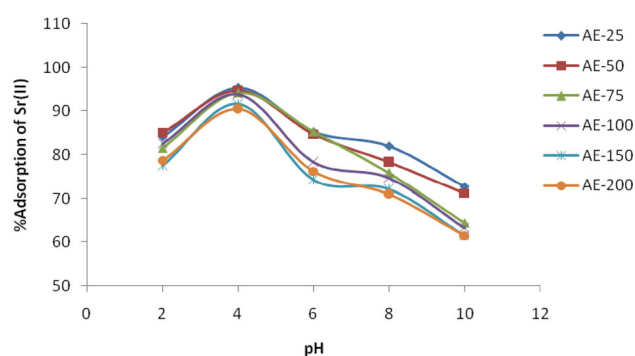


**Figure 10.** Influence of pH on Sr(II) adsorption.

(0.05%) was prepared by dissolving 50 mg of arsenazo(III) in 100 ml of deionized water.

### 3.9 Influence of pH

The pH of the solution is the most crucial parameters influencing the adsorption of the metal ion. The optimum pH conditions for the removal of Sr(II) sorption were determined using 50 mg of ethylene diamine-modified AGE-EGDMA polymeric beads added to 10 ml of 20 mg l<sup>-1</sup> of Sr(II) solution with pH ranging from 2 to 10. The residual concentration of strontium was measured by a spectrophotometer using the arsenazo(III) complexing agent. Figure 10 depicts the influence of pH on the adsorption of strontium.

The experimental data reveal that the maximum adsorption of Sr(II) was achieved at pH 4 (95.3% for AE-25; 94.8% for AE-50; 94.2% for AE-75; 93.8% for AE-100; 91.7% for

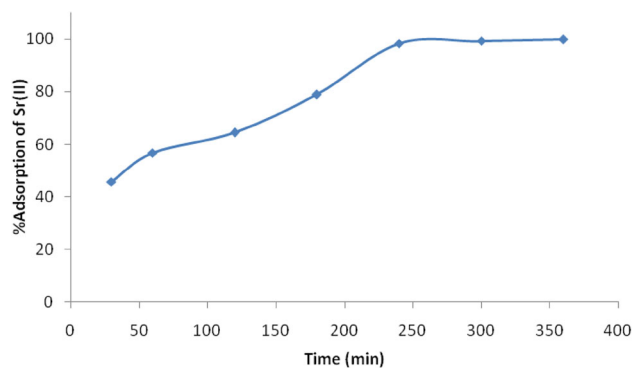


**Figure 11.** Effect of the contact time on Sr(II) adsorption.

AE-150 and 90.5% for AE-200) which indicated that a high affinity of Sr(II) ions was predominant at pH 4. Almost 88% of adsorption of the Sr(II) ion took place at pH 2. The adsorption efficiency of strontium(II) decreases with an increase in pH 4–10. At higher pH, Sr(II) adsorption efficiency was comparatively lower due to hydrogen bonding with the polymer [15]. In demineralized water, distribution of strontium species present in the form of  $\text{Sr}^{2+}$  at the pH range 1 to 11 and a very negligible  $\text{Sr}(\text{OH})^+$  species, which increases its concentration above pH 10. Hence, in the range of pH 6 to 8, strontium(II) was found in the form of  $\text{Sr}^{2+}$  [16]. At lower pH, the strong acidity replaced the adsorbed Sr(II) ions by  $\text{H}^+$ , which decreases the adsorption capacity of strontium [17]. Therefore, for further adsorption experiments, pH 4 was selected.

### 3.10 Effect of contact time

The optimum sorption time of Sr(II) ions was studied by applying the following procedure. Fifty milligrams of chemically modified AGE-EGDMA polymeric beads were shaken with 10 ml of Sr(II) solution ( $20 \text{ mg l}^{-1}$ ) at different sorption times (30, 60, 120, 180, 240 and 360 min) at pH 4. The concentration of Sr(II) ions in the solution was determined by a spectrophotometer using a recommended procedure. The results obtained from this study are presented in figure 11.

It can be seen that the adsorption percentage quickly increases with an increase in contact time. This result showed that the adsorption process was rapid. As demonstrated in figure 11, the optimum adsorption contact time was 240 min and about half of the time for saturation of chemically modified AGE-EGDMA polymeric beads was < 60 min. These data also showed that Sr(II) uptake on these polymeric beads reflected good accessibility of the sorption site in the polymeric beads. The adsorption time is an important factor that affects the efficiency of strontium ions by the polymeric beads in the aqueous phase. Therefore, an adsorption equilibrium time of 240 min for polymeric beads was selected and used for all further studies.

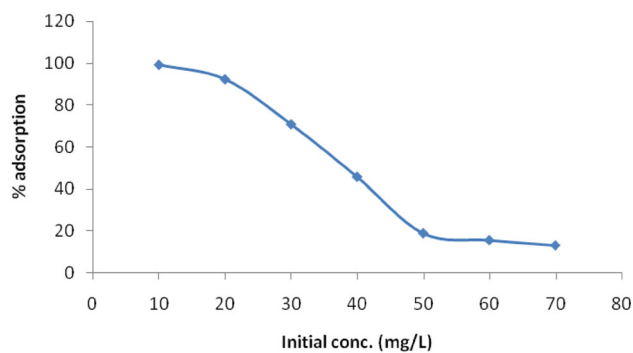


**Figure 12.** Effect of the initial concentration on Sr(II) adsorption.

### 3.11 Effect of metal ion concentration

The effect of metal ion concentration is the second most important factor that affects the metal ion adsorption. The effect of the metal ion concentration on the metal adsorption using polymeric beads was investigated. In this experiment, 50 mg of ethylene diamine modified AGE-EGDMA polymeric beads were added to 20 ml capacity test tubes containing 10 ml (10, 20, 30, 40, 50, 60 and 70 ppm) of each metal ion in pH 4 buffer solution. The adsorption of Sr(II) ions on AGE-EGDMA polymeric beads (50 mg) was tested. The experimental results are shown in figure 12.

As shown in figure 12, the maximum adsorption was achieved for 10 ppm solution i.e., 99.2%, whereas only 13.3% was obtained for the 70 ppm solution. The amount of Sr(II) adsorption decreases with an increase in the metal ion concentration. The adsorption percentage of Sr(II) was almost constant for strontium concentration ranging from 50–70 ppm. This was mainly due to the adsorption sites on adsorbents which were occupied by metal ions.

### 3.12 Effect of adsorbent dose

The effect of adsorbent dose was investigated with 40 ppm of Sr(II) metal ion solution. Ten millilitres of (40 ppm) strontium solution was added to six different 20 ml capacity glass test tubes. To these glass tubes, different amounts of adsorbents (20, 40, 60, 80, 100 and 120 mg) were added and kept aside at room temperature for 4 h. Supernatant layers from each test tube were removed and analysed using a UV spectrometer. The results are presented in figure 13.

The effect of the amount of AGE-EDMA polymeric beads on the removal of Sr(II) was investigated. The obtained results showed that the removal efficiency increased with an increase in the amount of adsorbent dose. It was clearly understood that the adsorption capacity of polymeric beads depends on the surface activity. Hence, greater concentration of the adsorbent contained more adsorptive sites. Until now, various kinds of adsorbents have been employed for the removal of strontium from contaminated water. However, the polymer-supported 18-crown-6-ether was hardly used for the removal

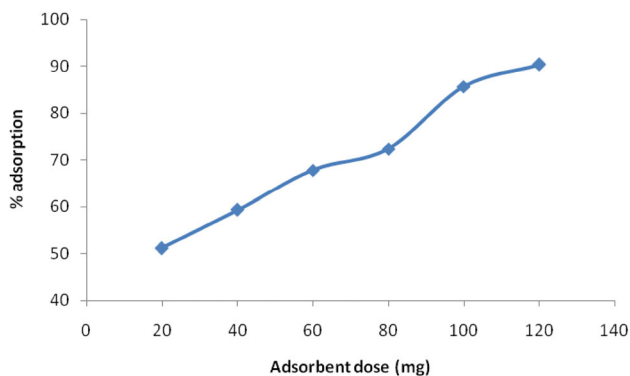


**Figure 13.** Effect of the adsorbent dose on Sr(II) adsorption.

of strontium from contaminated water. About 90% of Sr(II) removal efficiency was achieved using 150 mg of polymer-supported 18-crown-6-ether [18].

### 3.13 Adsorption kinetics

Adsorption kinetic models are used to investigate the controlling mechanism of the adsorption process. The kinetic model also describes the rate of the removal of metal ions from the aqueous phase which is one of the most important characteristics that defines the efficiency of adsorption. The efficiency of adsorption is determined using the kinetics of uptake of metal ions by the adsorbent. It is nothing but the study of the rate of metal ions uptake by the adsorbent. The equilibrium is determined by the distribution of a solute between solid-liquid phases and also by determining the feasibility and capacity of the sorbent for adsorption. Currently, a number of kinetic models are used to explain the mechanism of adsorption progress. The pseudo-first-order and pseudo-second-order kinetic models are used to evaluate the kinetic mechanism and also tested to interpret the experimental data. The simplest and widely used Lagergren pseudo-first order equation is given below [19,20].

$$\log (q_e - q_t) = \log q_e - \frac{K_{ad}t}{2.303}, \quad (1)$$

where  $q_e$  is the mass of the metal adsorbed at equilibrium ( $\text{mg g}^{-1}$ ),  $q_t$  the mass of the metal adsorbed at time  $t$  ( $\text{mg g}^{-1}$ ) and  $K_{ad}$  is the first-order reaction constant ( $\text{l min}^{-1}$ ). The rate constants for the adsorption of strontium ions onto polymeric beads were determined by using the above Lagergren equation. The pseudo-first-order kinetic model considers that the rate of occupation of sorption sites is proportional to the number of unoccupied sites. The rate constant  $K_{ad}$  for the adsorption of chromium on beads was studied by using the initial metal ion concentration,  $40 \text{ mg l}^{-1}$ , and the results are presented in figure 14. The adsorption rate constant  $K_{ad}$  is calculated from the slope of the above plot. The correlation coefficient ( $R^2$ ) for the first-order rate constant is 0.876.

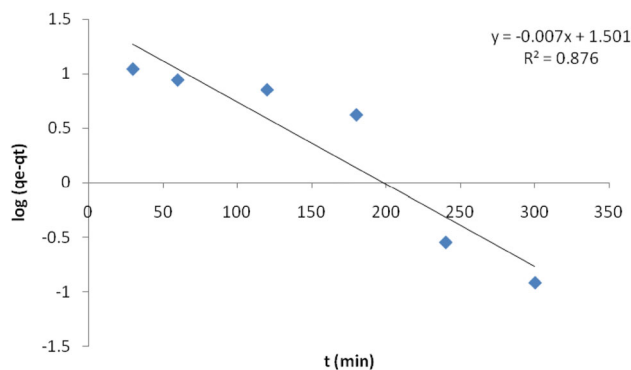


**Figure 14.** Pseudo-first-order kinetic plot for Sr(II) adsorption.

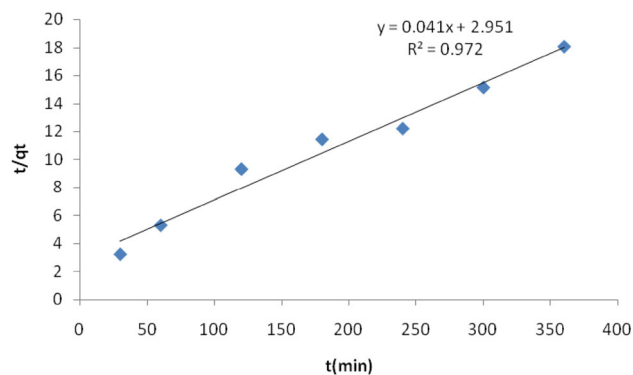


**Figure 15.** Pseudo-second-order kinetic plot for Sr(II) adsorption.

For the adsorption system, pseudo-second order kinetic expression is developed by Ho [21]. It assumes that the adsorption rate is controlled by chemical adsorption. The pseudo-second order rate equation describes equilibrium capacity. It depends on the concentration of either first-order reactants or second-order reactant. The pseudo-second order rate equation is presented as follows:

$$\frac{t}{q_t} = \frac{1}{K_{2ad}q_e^2} + \frac{t}{q_e}, \quad (2)$$

where  $K_{2ad}$  is the second-order reaction rate equilibrium constant ( $\text{g mg}^{-1} \cdot \text{min}^{-1}$ ) for the adsorption of Sr(II) on beads with a concentration of  $40 \text{ mg l}^{-1}$ . The kinetic plot of  $t/q_t$  vs.  $t$  for the adsorption of Sr(II) is shown in figure 15. As shown in figure 15, a plot of  $t/q_t$  vs.  $t$  provides a good straight line and gives a linear relationship for the applicability of the second-order kinetic model. The second-order rate constant  $K_{2ad}$  was calculated from the graph. The correlation coefficient ( $R^2$ ) for the second-order rate constant was 0.972 indicating that the results were fitted well with the pseudo-second-order kinetic model.

The mechanism of adsorption process is investigated by applying the intra-particle diffusion kinetic model [22] (equation (3)) and the result is shown in figure 16.

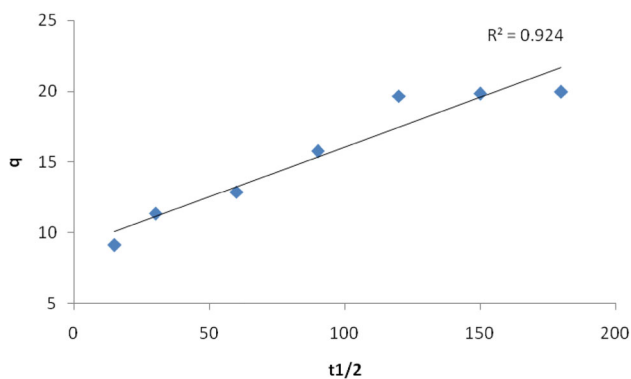


**Figure 16.** Intra-particle diffusion kinetic model.

$$q = K_i t + C, \quad (3)$$

where  $C$  is the intercept and  $K_i$  the intra-particle diffusion rate constant ( $\text{mg g}^{-1} \text{min}^{-1/2}$ ). It can be evaluated from the slope of the linear plot of  $q$  vs.  $t^{1/2}$ . When comparing the regression coefficients, the first-order rate expression and intra-particle diffusion model were not fully valid for the present system. However, a good agreement of experimental data with the second-order kinetic model was observed.

#### 4. Conclusions

In conclusion, resorcin[4]arene-functionalized macroporous poly(AGE-co-EGDMA) beads were successfully synthesized. These macroporous beads were used for the adsorptive removal of strontium(II) from the aqueous phase. The batch experiments were performed at pH ranging from 2–10. The effects of parameters such as pH, contact time, adsorbent dose and initial metal ion concentration were tested. The result showed that the maximum adsorption affinity (about 99%) was observed at pH 4 by functionalized macroporous poly(AGE-co-EGDMA), the optimum conditions for 50 mg of functionalized beads and 20 ppm Sr(II) were solution of pH 4 and adsorption time of 4 h at room temperature. The adsorption kinetic models, pseudo-first-order and pseudo-second-order kinetics were analysed. The correlation coefficient ( $R^2$ ) for pseudo-first-order and pseudo-second-order

kinetics was found to be 0.876 and 0.972, respectively. We propose that this resorcin[4]arene-functionalized macroporous poly(AGE-co-EGDMA) beads can effectively remove strontium ions from contaminated water.

#### References

- [1] NLM. Rickets. Available from: <http://www.nlm.nih.gov/medlineplus/ency/article/000344.htm>. Accessed on 8th Jan 2018
- [2] Mariangela G, Kaykioglu G, Belgiorno V and Lofrano G 2012 *Removal of emerging contaminants from water and wastewater by adsorption process*. In *emerging compounds removal from wastewater natural and solar based treatments* (Salerno: Springer) p 15
- [3] Nwafulugo F U, Adefila S S, Olawale A S and Ajayi O A 2014 *J. Environ. Sci. Water Res.* **3** 132
- [4] Wang J and Chen C 2009 *Biotech. Advan.* **27** 195
- [5] Won W, Kotte P, Wei A and Yeoung-Sang Y 2014 *Biores. Tech.* **160** 203
- [6] Liu C, Bai R and Hong L 2006 *J. Colloid. Interface Sci.* **303** 99
- [7] Liu Q, Xia B, Huang J, Liao J, Liu H, Ou B *et al* 2017 *Mater. Chem. Phys.* **199** 616
- [8] Liu Q, Li G, Tang Z, Chen L, Liao B, Ou B *et al* 2017 *Mater. Chem. Phys.* **186** 11
- [9] Duran A, Solak M and Tunel S A 2008 *J. Hazard. Mater.* **155** 114
- [10] Joanna K and Grzegorz S 2013 *Cent. Eur. J. Chem.* **11** 1723
- [11] Frechet J M 1993 *J. Macromol. Chem. Macromol. Symp.* **70** 289
- [12] Hoegberg A 1980 *J. Org. Chem.* **45** 4498
- [13] Matsushita Y and Matsui T 1993 *Tetra. Lett.* **34** 7433
- [14] Agrawal Y K and Jain R K 1979 *J. Chem. Eng. Data* **24** 250
- [15] Rongjian Y 2015 *Inter. J. Anal. Chem.* Article ID 425084 1
- [16] Yavari R, Huang Y D and Mostofizadeh A 2010 *J. Radioanal. Nucl. Chem.* **285** 703
- [17] Wang M, Xu L, Peng J, Zhai M, Li J and Wei G 2009 *J. Hazard. Mater.* **171** 820
- [18] Mane S T, Ponrathnam S and Chavan N N 2016 *J. Appl. Polym. Sci.* 42849
- [19] Lagergren S 1898 *Handlingar* **24** 1
- [20] Aksu Z 2002 *Process. Biochem.* **38** 89
- [21] Ho Y S and McKay G 1998 *Adsorpt. Sci. Technol.* **16** 243
- [22] Namasivayam C and Ranganathan K 1993 *Environ. Poll.* **82** 255